EBioMedicine 22 (2017) 181–190

Contents lists available at ScienceDirect

EBioMedicine

journal homepage: www.ebiomedicine.com

Research Paper

The Mechanism of Diabetic Retinopathy Pathogenesis Unifying Key Lipid Regulators, Sirtuin 1 and Liver X Receptor

Sandra S. Hammer [a], Eleni Beli [b], Nermin Kady [a], Qi Wang [a], Kiana Wood [a], Todd A. Lydic [a], Goldis Malek [c], Daniel R. Saban [c], Xiaoxin X. Wang [d], Sugata Hazra [e], Moshe Levi [d], Julia V. Busik [a,*], Maria B. Grant [b,**]

[a] Department of Physiology, Michigan State University, East Lansing, MI, United States
[b] Department of Ophthalmology, Indiana University School of Medicine, Indianapolis, IN, United States
[c] Department of Ophthalmology, Duke University School of Medicine, Durham, NC, United States
[d] Department of Medicine, University of Colorado, Aurora, CO, United States
[e] Department of Pharmacology, University of Florida, Gainesville, FL, United States

ARTICLE INFO

Article history:
Received 10 April 2017
Received in revised form 6 July 2017
Accepted 7 July 2017
Available online 11 July 2017

Keywords:
Diabetic retinopathy
Dyslipidemia
Liver X receptor
SIRT1
Glucose
Retinal inflammation
Bone marrow
Circulating angiogenic cells
Tumor necrosis factor alpha
Cholesterol metabolism
Reverse cholesterol transport
Cholesterol efflux
Retinal endothelial cells

ABSTRACT

Diabetic retinopathy (DR) is a complication secondary to diabetes and is the number one cause of blindness among working age individuals worldwide. Despite recent therapeutic breakthroughs using pharmacotherapy, a cure for DR has yet to be realized. Several clinical trials have highlighted the vital role dyslipidemia plays in the progression of DR. Additionally, it has recently been shown that activation of Liver X receptor (LXRα/LXRβ) prevents DR in diabetic animal models. LXRs are nuclear receptors that play key roles in regulating cholesterol metabolism, fatty acid metabolism and inflammation. In this manuscript, we show insight into DR pathogenesis by demonstrating an innovative signaling axis that unifies key metabolic regulators, Sirtuin 1 and LXR, in modulating retinal cholesterol metabolism and inflammation in the diabetic retina. Expression of both regulators, Sirtuin 1 and LXR, are significantly decreased in diabetic human retinal samples and in a type 2 diabetic animal model. Additionally, activation of LXR restores reverse cholesterol transport, prevents inflammation, reduces pro-inflammatory macrophages activity and prevents the formation of diabetes-induced acellular capillaries. Taken together, the work presented in this manuscript highlights the important role lipid dysregulation plays in DR progression and offers a novel potential therapeutic target for the treatment of DR.

1. Introduction

Diabetic retinopathy (DR) is the number one cause of blindness among working age adults. Despite recent advances using pharmacotherapy, a cure for DR has yet to be realized. The recent evidence from large clinical trials demonstrating a strong association between lipid abnormalities and DR progression provides a unique opportunity to uncover innovative pathogenic mechanisms in DR (Ferris et al., 1996; Lyons et al., 2004; Keech et al., 2005). Specifically, recent studies demonstrate that intensive control of cholesterol levels can significantly slow down DR progression in type 2 diabetic individuals (Keech et al., 2005; Klein et al., 1999; Du et al., 2013). Unlike macrovascular complications, the Diabetes Control and Complications Trial (DCCT), Epidemiology of Diabetes Interventions and Complications (EDIC) and the Action to Control Cardiovascular Risk in Diabetes (ACCORD) eye trials, as well as Blue Mountain Eye Study and the Wisconsin Epidemiologic Study of Diabetic Retinopathy (WESDR) studies did not find a direct correlation between the development of DR and circulating lipid levels, suggesting that retinal-specific mechanisms may be at play.

We have previously demonstrated that diabetic dyslipidemia promotes retinal vascular degeneration at several levels. First, changes in retinal-specific lipid metabolism can contribute to low-grade chronic inflammation resulting in endothelial cell injury (Opreanu et al., 2011). Second, there is inadequate repair of the injured retinal capillaries by bone marrow-derived (BMD) circulating angiogenic cells (CACs) (Chakravarthy et al., 2016). These cells are exquisitely sensitive to the damaging diabetic milieu and are adversely impacted by dyslipidemia. Finally, activated myeloid cells promote a pro-inflammatory environment in the retina (Chakravarthy et al., 2016; Hazra et al., 2013). Thus, retinal endothelial cell injury, activated myeloid cells and failed

* Correspondence to: Julia V. Busik, Michigan State University, 567 Wilson Rd, Biomed Phys Sci Room 3178, East Lansing, MI 48824, United States.
** Correspondence to: Maria B. Grant, Indiana University School of Medicine, R3-C426D, Indianapolis, IN 4602, United States.
E-mail addresses: busik@msu.edu (J.V. Busik), mabgrant@uab.edu (M.B. Grant).

http://dx.doi.org/10.1016/j.ebiom.2017.07.008

attempts by CACs to repair injured retinal capillaries collectively result in progression to the vaso-degenerative stage of the disease. The role of diabetes-induced cholesterol metabolic abnormalities at each of these levels is addressed in this study.

Cholesterol metabolism of retina and brain is unique among peripheral organs due to the tight barrier separating them from systemic circulation (Dietschy and Turley, 2001; Fliesler and Bretillon, 2010). In the brain, cholesterol is exclusively supplied by local synthesis. Retina also synthesizes cholesterol, but unlike brain, retina has mechanisms for cholesterol delivery from the systemic circulation (Fliesler et al., 1993; Pikuleva and Curcio, 2014; Tserentsoodol et al., 2006). In healthy retina, most of the blood-borne cholesterol is delivered via the outer blood retinal barrier (BRB) located at the RPE layer (Fliesler and Bretillon, 2010). In the diabetic retina, an abnormal increase in cholesterol uptake is observed in the inner BRB (retinal microvasculature) in addition to the outer BRB (Fliesler et al., 1993; Zheng et al., 2012). Retinal vasculature and RPE play an important role in cholesterol elimination. Unlike most peripheral tissues where HDL-mediated reverse cholesterol transport (RCT) represents the major pathway of cholesterol elimination, both RCT and metabolism of cholesterol to more soluble oxysterols, are active in the retina (Mast et al., 2011; Pikuleva and Curcio, 2014; Tserentsoodol et al., 2006). The first step of RCT, cellular efflux of cholesterol, is controlled by ATP binding cassette transporters ABCA1 and ABCG1, scavenger receptor class B type I (SR-BI), cluster of differentiation 36 (CD36), and caveolin-1, all expressed in the retina (Duncan et al., 2009; Tserentsoodol et al., 2006). The second elimination pathway, metabolism of cholesterol to more soluble oxysterols, is realized via cytochrome P450 enzymes (CYPs). The oxysterol profile of the retina suggests that all known pathways of cholesterol metabolism in extraocular organs are operative in the retina.

Oxysterols serve as endogenous ligands of liver X receptors (LXRα (NR1H3)/LXRβ (NR1H2)) (Janowski et al., 1996). In addition to their established role in cholesterol metabolism (Janowski et al., 1999), LXRs also suppress inflammatory gene expression, thus controlling immune response and inflammation (Huang et al., 2011; Ogawa et al., 2004; Pascual et al., 2005). Importantly, LXR null mice, even in the absence of hyperglycemia, present with pathological changes seen in the diabetic retina, dramatically reduced CAC function and increased levels of activated macrophages (Hazra et al., 2012). Another key metabolic regulator, Sirtuin 1 (SIRT1), was recently shown to exert its beneficial effect through LXR-dependent mechanisms (Li et al., 2007). SIRT1 is the mammalian ortholog of yeast *Sir2* gene that has been shown to play a role in aging, apoptosis, neural protection, glucose metabolism and neural development (Miranda et al., 2015; Purushotham et al., 2009; Wang et al., 2011). SIRT1 interacts with LXR to promote its deacetylation at a single conserved lysine (K432 in LXRα and K433 in LXRβ) adjacent to the ligand-regulated activation domain, leading to LXR activation (Li et al., 2007). Via LXR activation, SIRT1 promotes insulin secretion, reduces glucose tolerance and decreases body weight (Zabolotny and Kim, 2007; Purushotham et al., 2009; Wang et al., 2011). Importantly, SIRT1 is critical to vascular health (Kitada et al., 2016). High glucose adversely influences CAC function by reducing SIRT1, while increasing SIRT1 in CACs of diabetic origin corrects their dysfunction (Balestrieri et al., 2008, 2013; Yuen et al., 2012). Animal and in vitro studies have demonstrated the importance of SIRT1 regulation of inflammation (Zabolotny and Kim, 2007; Howitz et al., 2003; Liang et al., 2009). Activation of SIRT1, followed by LXR deacetylation resulted in inhibition NFκB activity induced by high-fat diet, and sustained repression of inflammatory genes (Zeng et al., 2013). By contrast, SIRT1-KO mice on a high-fat diet were prone to liver inflammation (Purushotham et al., 2009). In primary macrophages, deficiency of SIRT1 decreased the induction of the LXR target gene, ABCA1, impairing cholesterol export. Activation of SIRT1 enhanced LXRα, activity and ABCA1 and ABCG1 expression (Li et al., 2007). SIRT1-LXRα axis is also significantly reduced in U937 cells during foam cell formation (Zeng et al., 2013). Finally, decreased SIRT1 levels have recently been implicated in the pathogenesis of microvascular complications, specifically DR (Kowluru et al., 2014). The interplay of SIRT1 with LXR in the pathogenesis of DR has not been previously investigated and represents the focus of this study.

2. Materials and Methods

2.1. Animal Studies

All animal procedures were in compliance with the National Institutes of Health (NIH) *Guide for the Care and Use of Laboratory Animals*, and with the Association for Research in Vision and Ophthalmology *Statement for the Use of Animals in Ophthalmic and Vision Research*. Diabetic, Lepr$^{db/db}$ (B6.BKS(D)-*Lepr$^{db/J}$*) and their corresponding controls Lepr$^{db/m}$, were purchased by Jackson laboratories (Coleman, 1978). The procedures were carried out in accordance with the guidelines of the Indiana University School of Medicine, Institutional Animal Care and Use Committee (IACUC). For experiments with GW3965 treatment 8-week-old male db/db mice were fed a chow diet mixed with GW3965 at a dose of 10 mg/kg body weight/day for 12 weeks. The type 2 diabetic BBZD rat model (4 months diabetes) was used to measure retinal cholesterol metabolism (Tirabassi et al., 2004; Busik et al., 2009).

2.2. Cell Culture and Treatment

Primary cultures of human retinal endothelial cells (HRECs) were prepared from the retinas provided by National Disease Research Interchange (Philadelphia, PA, USA) as previously described (Wang et al., 2014, 2016b). Characteristics of the donors are summarized in Wang et al. (2014). Bovine retinas were isolated from eyes donated by the Michigan State University Meat Laboratory. BRECs were isolated and validated according to a previously published protocol (Antonetti et al., 1998). BREC identity was confirmed morphologically and by response to vascular endothelial growth factor (293-VE), Anti-Von Williebrand Factor immunocytochemistry (ab6994) and LDL uptake assay (ab133127; Abcam; Cambridge, MA) (Stewart et al., 2011). BREC were cultured in 10% Fetal Bovine Serum (FBS) Complete Media with 1% Antibiotic/Antimycotic (AA) (Gibco; ThermoFisher; Waltham, MA). Passages 4–8 were used for all experiments. Prior to treatment, cells were grown to 80% confluency and serum starved overnight (12–18 h). BREC were serum starved in 1% Fetal Bovine Serum Complete media. Cells were treated with diabetic relevant stimuli tumor necrosis factor alpha (TNFα) for 24 h (10 ng/ml) (2279-BT; R&D Systems) (Wang et al., 2016a). In order to activate the SIRT1-LXR pathway, BRECs were treated with LXR activator, DMHCA (0.1 μM/1 μM) (700125P; Avanti Polar Lipids; Alabaster, AL), GW3965 (10 μM) (10054; Cayman Chemical; Ann Arbor, MI) or SIRT1 activator SRT1720 (1 μg) (S1129; Sellechem; Houston, TX) for 24 h (Mitchell et al., 2014; Kratzer et al., 2009).

2.3. Real-time Quantitative PCR

RNA from HREC and BREC was isolated according with the RNeasy mini kit (74106; Qiagen, Valencia, CA) according to manufacturer's instructions. First-strand complementary DNA was synthesized from isolated RNA using SuperScript II reverse transcription (18064014; Invitrogen). Prepared cDNA was mixed with 2× SYBR Green PCR Master Mix (4309155; Applied Biosystems) and various sets of gene-specific forward and reverse primers (LXRα, LXRβ, ABCA1, ABCG1, IL1β, IL-6, SIRT1 and SREBP-1c (Integrated DNA Technologies; Coralville, IA) and subjected to real-time PCR quantification using the ABI PRISM 7700 Sequence Detection System (Applied Biosystems). Primer sequences are identified in Table 1. All reactions were performed in triplicate. Cyclophilin A was used as a control, and results were analyzed using the comparative Ct method and Ct values were normalized to Cyclophilin A levels. Data is shown as normalized relative to control

Table 1
Qualitative real time PCR primer sequences.

Primer name	Forward (5′ to 3′)	Reverse (5′ to 3′)
Cyclophilin A	GAG CAC TGG AGA GAA AGG ATT T	GAC TTG CCA GTA CCA TTA T
LXRα	GAG AGG CTG CAA CAC ACA TA	AGG CTC ACC AGT TCA TCA G
LXRβ	GAA GGT GAA GGT GTC CAG TT	GTC GGA GAA GGA GCG TTT ATT
ABCA1	CTC AGT GGG ATG GAT GGT AAA G	TGG CAA TCA GCA GTC TCT TC
ABCG1	AGA CCT GCC ATT TCC AGA AG	GAT GAG ACG CAG GGA GAT AAA G
SIRT1	CCC TGA AAG TAA GAC CAG TAG C	GTG AGG CAA AGG TTC CCT ATT A
IL-1β	CTA TTC TCT CCA GCC AAC CTT C	CTC GTC ACT GTA GTA AGC CAT C
IL-6	CCA GAA CGA GTA TGA GGG AAA TC	TTG TGG CTG GAG TGG TTA TTA G
SREBP-1	GAC TAC ATC CGC TTC CTT CAG	CCA GGT CCT TCA GCG ATT T

levels or as non-normalized raw expression levels. Mouse eyes were enucleated and retinas were dissected. RNA from retinas and bone marrow derived macrophages was isolated using the RNeasy mini Kit (Qiagen). Reverse transcription was done using the Superscript VILO cDNA Synthesis Kit (11754050; Life Technologies). Real-time PCR was performed on an ABI PRISM 7900HT Sequence Detection System, using TaqMan Fast Universal PCR Master Mix (2×) (4352042; Life Technologies) and TaqMan primer/probe gene expression assays. The expression of β-2 microglobulin and cyclophillin-β were used as endogenous controls. The relative copy number was calculated as 1/POWER(2,ΔCT)*100.

2.4. Acellular Capillaries

The sensory retina was isolated by gently separating it from pigment epithelium and choroid using a #00 paint brush under a dissecting microscope. Capillaries prepared using elastase digestion, and stained with hematoxylin and periodic acid–Schiff as detailed in Veenstra et al., 2015 and previously described (Kern et al., 2000; Laver et al., 1993; Opreanu et al., 2011; Veenstra et al., 2015). Acellular capillaries were quantified in a masked, randomized manner by three independent examiners (Laver et al., 1993; Opreanu et al., 2011; Veenstra et al., 2015).

2.5. Oxysterol Measurement

Retinal samples were subjected to total lipid extraction by a monophasic chloroform/methanol/water mixture simultaneously extract cholesterol, oxysterols, and cholesteryl esters (Lydic et al., 2014). Oxysterols were analyzed by LC-MS/MS on an ultra- high resolution/accurate mass LTQ-Orbitrap velos platform (Thermo Scientific) coupled to an Agilent 1260 capillary HPLC. LC gradient conditions were based on LIPID MAPS LC-MS/MS methodology for sterol and oxyterol analysis modified by use of a ProntoSIL C18AQ 3 μ 120 Å, 0.2 mm × 50 mm capillary LC column (nanoLCMS Solutions) at a flow rate of 2 μl/min (Mcdonald et al., 2007). The column was directly coupled to a Nano-ADVANCE nESI source (Bruker-Michrom). Chromatographic peak alignment, compound identification, and quantitation were performed with Maven software in conjunction with an in-house database of metabolite identities and retention times (Melamud et al., 2010). Cholesterol, cholesteryl esters, and other nonpolar lipids were analyzed by direct infusion nESI ultra high resolution/accurate mass MS and MS/MS as previously described by us (Lydic et al., 2014).

2.6. Bone Marrow Derived Macrophages (BMDM)

Macrophages were derived from cultures of murine bone marrow cells (2.5×10^6 cells/well, 3 ml/well) in 6-well plates with macrophage growth media: RPMI-L929 (Sigma-Aldrich, St. Louis, MO) supplemented with 10% heat inactivated donor equine serum (HyClone, GE Healthcare Life sciences, Pittsburgh, PA), 5% heat inactivated fetal bovine serum (Gibco™, Thermo Fischer), 15% L929-conditioned media, 1×–L-glutamine (Gibco™) and 1× antibiotics (Gibco™). Media changes were performed at 3, and at day 6. On Day 7, macrophages were stimulated for the next 18 h with LPS (100 ng/ml, Sigma) and murine IFN-γ (40 ng/ml, life sciences) or with metabolic stimuli consisting of 30 mM glucose (using 45% glucose solution, Gibco™), 10 nM insulin (Humulin, R, Lilly), 400 μM palmitate (N-16-A, Nu-Chekprep, Elysian, MN) according to (Kratz et al., 2014) 10 μM GW3965 (Sigma) was added with the stimulation for 18 h. Control medium was RPMI – 1640 enriched with 10% heat inactivated donor equine serum, 5% FBS, antibiotics, L-glutamine and 11.1 mM glucose. In all media, glucose was adjusted to 11.1 mM or 30 mM with the addition of 45% glucose solution (Gibco™). At the end of the experiment, cells were lysed and RNA was extracted as described above.

2.7. siRNA Transfection

SIRT1 siRNA transfections were conducted using Amaxa Human Coronary Artery Endothelial Cells (HCAEC) Nucleofector Kit (V4XP-5024; Lonza; Cologne, Germany). SIRT1 directed oligomers and control siRNA oligomers were designed using Custom Stealth RNAi siRNA tool (ThermoScientific). siRNA sequences are identified in Table 2. Two different sets of SIRT1 directed siRNA oligomers were used but SIRT1 knockdown efficiency was only achieved using the sequences demonstrated in Table 2. Supplemental Fig. 1 demonstrates the SIRT1 siRNA oligomers that were unsuccessful in blocking SIRT1 mRNA levels in BREC.

2.8. Western Blot Analysis

BREC were cultured and treated as necessary. Lysates were collected by scraping cells using cold 1× radioimmunoprecipitation assay buffer (RIPA) with protease and phosphatase inhibitor (89900; Thermo Scientific). Bradford protein assay was used to measure total protein level and equal amounts of protein (25 μg) were loaded in each well. 10% Bis-Tris NuPAGE gels were transferred to 0.2 μm nitrocellulose membranes. Membranes were probed overnight with ABCA1 (ab18180; Abcam), and β-actin antibodies (4970; Cell signaling technology: Danvers, MA). β-actin was used as a loading control. Blots were analyzed using the LI-COR Odyssey imaging and quantification system.

2.9. Enzyme Linked Immunosorbent Assay (Elisa)

BREC were grown in 24-well dishes until 80% confluent. Cells were treated as mentioned above (cell culure and treatment), and media was collected for analysis. IL6 and IL1β protein levels were measured via ELISA (IL6, ab205080, abcam; IL1β, ESS0027, Thermo Scientific) treatment with TNFα and/or LXR activator, DMHCA. Manufactures instructions were followed for each kit.

2.10. Circulating Angiogenic Cell (CAC) Migration

CAC function was determined by measuring migration using the QCM™ chemotaxis 5 μM 96-well cell migration assay (Chemicon International, Inc.) as per the manufactures instructions. Migratory response to stromal derived factor-1 (SDF-1) or VEGF was expressed as arbitrary fluorescence unit (AFU) (Balaiya et al., 2014).

Table 2
Control and SIRT1-directed siRNA oligomer sequences.

Primer name	Primer number	Sequence (5′ to 3′)
SIRT1	314004G12	(RNA)- CAA ACU UGA AGA AUG GUC UUG GGU C
	314004H01	(RNA)- GAC CCA AGA CCA UUC UUC AAG UUU G
Control	314004H02	(RNA)- GAC GAA CCA UUA UUC AAC UGC CUU G
	314004H03	(RNA)- CAA GGC AGU UGA AUA AUG GUU CGU C

2.11. Statistics

A Student *t*-test was used for comparisons between two groups. One-way ANOVA, followed by the Tukey post hoc test, was used for multiple comparisons. All values are expressed as mean ± SEM. A value of $p < 0.05$ was considered to be statistically significant. Statistical tests were performed using statistics software (GraphPad Software; La Jolla, CA).

3. Results

3.1. Diabetes Leads to Significant Decrease in LXRα, LXRβ and SIRT1 Levels in Retina and Retinal Cells

To determine the effect of diabetes on SIRT1-LXR axis, retinas from $Lepr^{db/db}$ 10-month diabetic mice were isolated and LXRα and SIRT1 mRNA expression levels were compared to their corresponding $Lepr^{db/m}$ controls. TNFα expression was used to confirm increased inflammatory cytokine expression in diabetic retina (Fig. 1a). As shown in Fig. 1a, diabetic retinas had significantly decreased LXRα expression level as compared to control. We next determined LXR and SIRT1 expression levels in human retinal endothelial cells (HRECs) isolated from previously characterized (Wang et al., 2016b) diabetic human donor tissue with confirmed dyslipidemia and upregulation of pro-inflammatory markers (Wang et al., 2016b). LXR and SIRT1 expression levels were significantly decreased in HREC isolated from diabetic retinas compared to non-diabetic donor tissue, confirming that the SIRT1/LXR signaling pathway is downregulated during diabetes (Fig. 1b). LXR isoforms, α and β, were expressed at similar levels in HREC ($LXR\alpha = 0.007 \pm 0.002$, $LXR\beta = 0.004 \pm 0.001$).

3.2. Retinas From T2D Rats Have Increased Levels of Cholesterol Esters and Decreased Levels Oxysterols

To determine the effect of diabetes on retinal cholesterol metabolism, T2D BBZDR rat model was used for lipid analysis. As shown in Fig. 1C, oxysterol levels were decreased by 64% ($p < 0.05$) and total cholesteryl ester abundance was increased in T2D retinas compared to controls. Since diabetes induced a significant decrease in LXR activators oxysterols, these data suggest that LXR signaling and activation of downstream targets will be impaired in diabetic tissue.

3.3. LXR Agonism Prevents the Development of Acellular Capillaries in db/db Mouse Model

As all the components of SIRT1/LXR axis were downregulated in diabetic retinas and retinal cells, we next determined if pharmacological activation of LXR could correct retinal vascular damage induced by diabetes. LXR activator GW3965 was administered to $Lepr^{db/db}$ diabetic mice for 12 weeks, and diabetes-induced retinal vascular damage was accessed. Diabetes induced an increase in the formation of acellular capillaries in $Lepr^{db/db}$ 10-month diabetic mice as compared to non-diabetic $Lepr^{db/m}$ controls, while GW3965 prevented diabetes-induced vascular damage (Fig. 1d).

3.4. LXR Activation Restores CAC Cell Function in Diabetic Animals

Retinal vascular damage in diabetes is the combination of endothelial cell injury and failed attempts at repair by dysfunctional CACs (Chakravarthy et al., 2016). As systemic treatment with GW3965

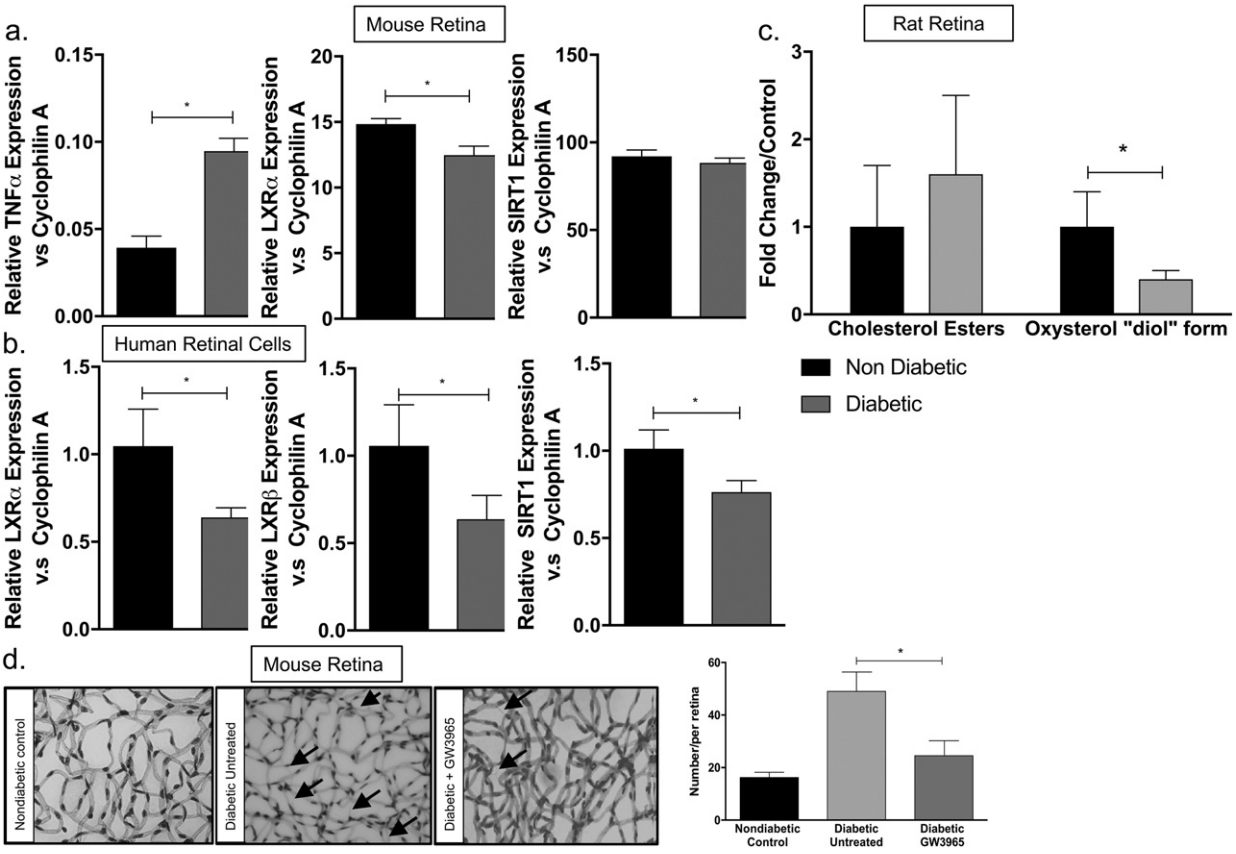

Fig. 1. Diabetes leads to a significant decrease in retinal LXR-SIRT signaling axis. (a) Retinas isolated from diabetic mice (10 months) have elevated TNFα expression levels, and decreased levels of LXRα when compared to non-diabetic animals (n = 6). (b) HREC isolated from diabetic patients have decreased levels of LXRα, LXRβ and SIRT1 when compared to non-diabetic donors (n = 3). TNFα, LXRα, LXRβ and SIRT1 expression levels were analyzed via qRT-PCR analysis. (c) Retinas from T2D rats have increased levels of cholesterol esters and decreased levels of natural LXR agonists oxysterols (n = 9). (d) Treatment with GW3965 an LXR agonist, for 12 weeks prevented the formation of acellular capillaries in db/db mice (right panel) when compared to diabetic untreated mice (middle panel) (n = 6). *$p < 0.05$.

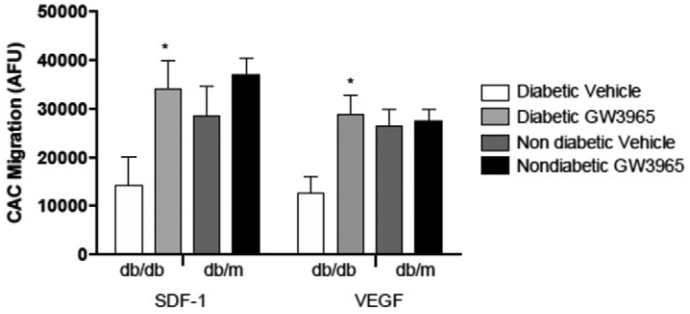

Fig. 2. LXR activation restores CAC cell function in diabetic animals. CAC cell function was determined by measuring CAC migration. Diabetes (10 months) (white bars) impairs CAC migration in response to SDF-1 and VEGF when compared to nondiabetic controls (dark grey bars). Treatment with GW3965 significantly improves CAC migration in response to SDF-1 and VEGF in diabetic mice (light grey bars) when compared to untreated diabetic mice (white bars) (n = 6). *p < 0.05.

could affect both retina and CACs, we next examined the effect of GW3965 on CAC migration. Diabetes induced a decrease in CAC migration in Lepr$^{db/db}$ 10-month diabetic mice as compared to non-diabetic controls. GW3965 increased in CAC migration in response to SDF-1 (Fig. 2).

3.5. LXR Activation Reduces Pro-inflammatory Cytokine Expression by Macrophages

Inflammation has a well-established role in DR pathogenesis and bone marrow-derived myeloid cells could contribute to the inflammatory phenotype (Hu et al., 2013). We next determined if LXR activation can affect macrophage function. Bone marrow derived macrophages were stimulated using LPS and IFN-γ in the presence or absence of 10 μM of the LXR agonist, GW3965. LPS and IFN-γ stimulation induced a strong inflammatory response as shown by IL-1β (Fig. 3a) and IL-6 (Fig. 3b) upregulation, while LXR activation inhibited this inflammatory response.

To mimic the effect of diabetes, bone marrow derived macrophages were challenged with metabolic stimuli (30 mM glucose, 10 nM insulin and 400 μM palmitate) in the presence or absence of 10 μM LXR agonist, GW3965 (Kratz et al., 2014). The metabolic stimuli, reduced ABCA1 mRNA expression (Fig. 3c), a target of the LXR pathway, and significantly increased IL-6 mRNA expression (Fig. 3d). LXR activation increased ABCA-1 expression and at the same time downregulated the induction of IL-6.

3.6. Pro-inflammatory Cytokines Significantly Decrease Expression of LXRα and RCT Genes in Bovine Retinal Endothelial Cells (BREC)

Retinal endothelial cells are exposed to cytokines produced by both retinal cells and bone marrow derived myeloid cells. To mimic the pro-inflammatory conditions found in the diabetic retina and their effects on LXR and RCT genes, BREC were treated with 10 ng/ml TNFα for 24 h. TNFα caused a significant decrease in LXRα but not LXRβ levels (Fig. 4a). Additionally, TNFα stimulation caused a significant decrease in the ATP-binding cassette transporters, ABCA1 and ABCG1.

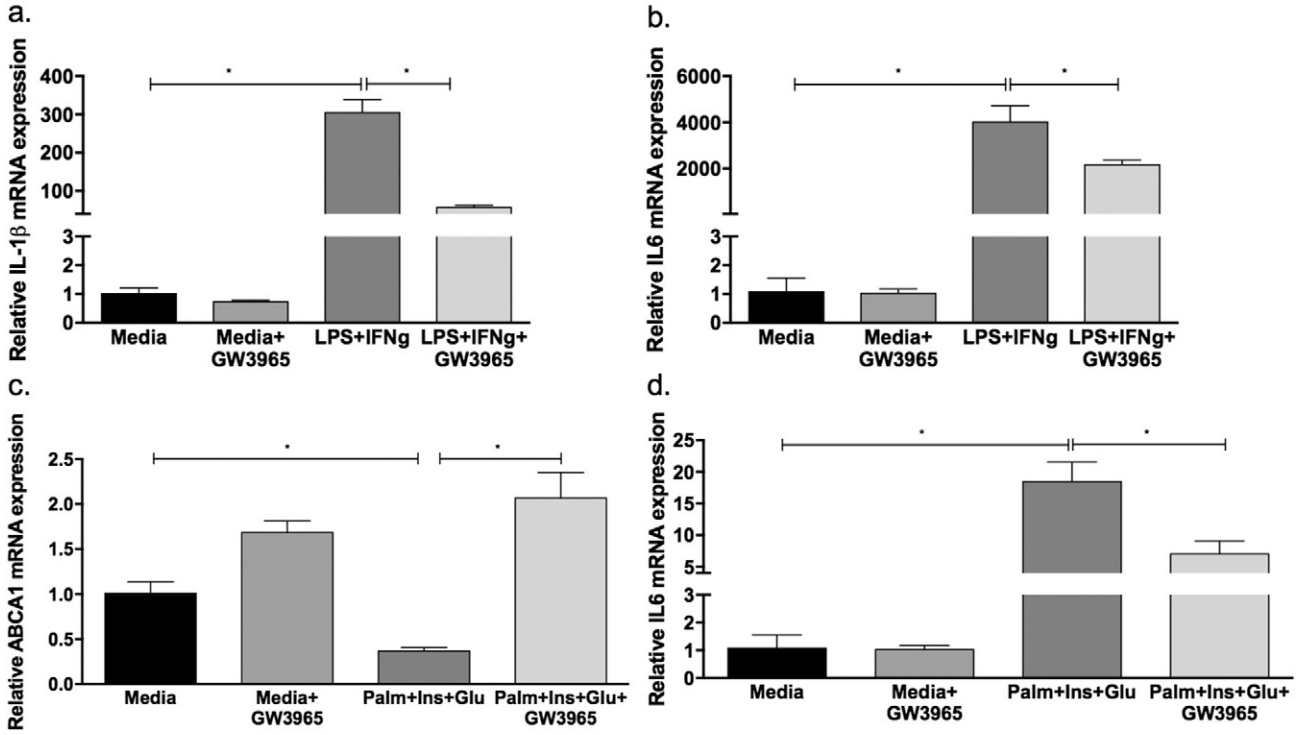

Fig. 3. LXR activation reduced proinflammatory expression stimulated by bone marrow-derived macrophages. qRT-PCR was performed BM-derived macrophages stimulated with (a, b) 100 ng/ml LPS and 40 ng/ml IFN-γ (c, d) 30 mM glucose, 10 nM insulin and 400 μM for 18 h in the absence or presence of 10 μM GW3965. (a) IL-1β, (b, d) IL-6 (c) ABCA1 mRNA relative expression (n = 3 per group). met = metabolic stimuli. *p < 0.05.

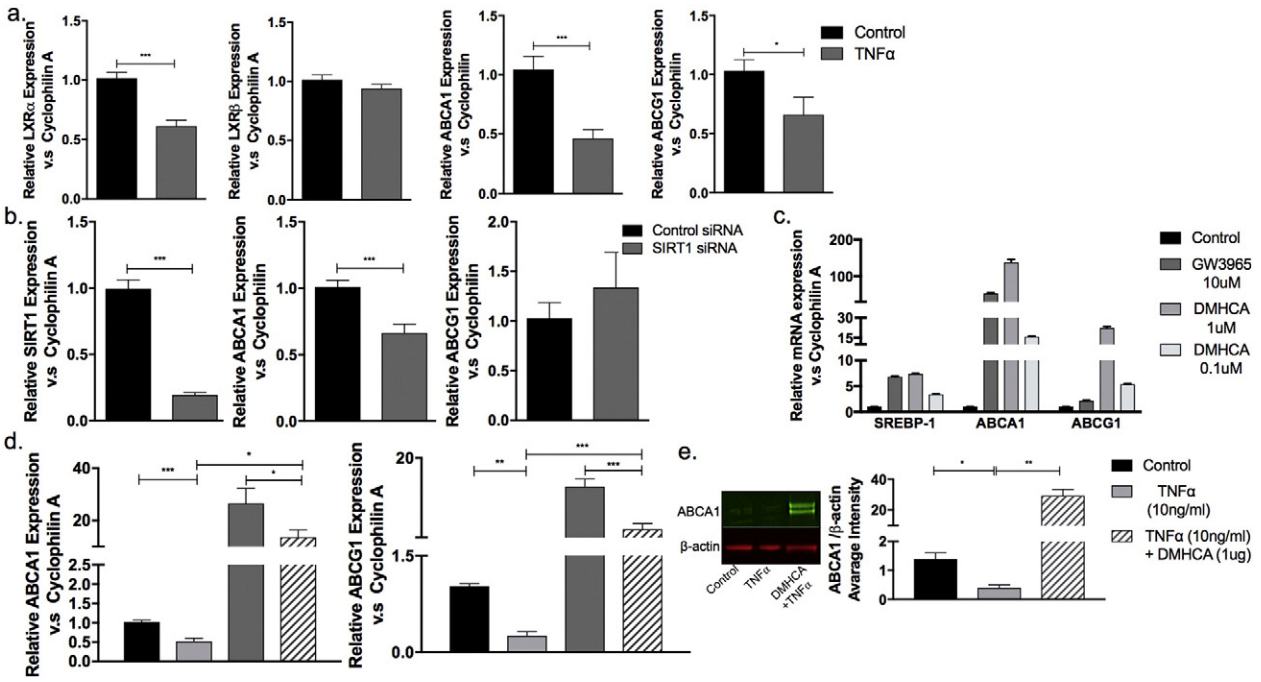

Fig. 4. TNFα causes a decrease in LXRα and reverse cholesterol transport genes in bovine retinal endothelial cells (BREC). BREC were treated with TNFα (10 ng/ml), SRT1720 (1 μM) or DMHCA (1 μM) for 24 h. (a) Treatment with TNFα caused a significant downregulation of LXRα, ABCA1, and ABCG1 (n = 12). (b) SIRT1 siRNA significantly decreases ABCA1 mRNA levels. BREC were treated with 100 nM control or SIRT1 siRNA for 48 h (n = 6). (c) LXR activators, GW3965 and DMHCA, effect on SREBP-1 mRNA levels. BREC were treated with either 10 μM GW3965, 1 μM DMHCA, or 0.1 μM DMHCA for 24 h (n = 3). (d) LXR activation blocks TNFα-induced ABCA1 and ABCG1 downregulation. ABCA1 and ABCG1 were significantly decreased in BREC treated with TNFα (n = 6). LXR activator, DMHCA inhibited TNFα-induced ABCA1, and ABCG1 downregulation (n = 6). (e) Western blot analysis of ABCA1 in BREC treated with TNFα ± DMHCA. β-actin was used as loading control (n = 3). Data analyzed via qRT-PCR. Cyclophilin A was used as a loading control. ***p < 0.001 **p < 0.01, *p < 0.05.

3.7. SIRT1 Knockdown Significantly Decreases Expression of ABCA1

SIRT1 has been shown to activate LXR via deacetylation. Subsequently, LXR activation promotes ABCA1 and ABCG1 expression (Kalaany and Mangelsdorf, 2006). In order to address the involvement of SIRT1 in increasing ABCA1 and ABCG1 in BRECs, loss of function studies were conducted using SIRT1-directed siRNA (Supplemental Table 2). Administration of 100 nM SIRT1 siRNA caused a significant decrease in ABCA1 levels but not ABCG1 levels when compared to cells treated with non-specific control siRNA (Fig. 4b). Inhibition of SIRT1 with SIRT1-directed siRNA did not affect LXRα/β expression levels.

3.8. LXR Activation via DMHCA Treatment Blocks TNFα-Induced ABCA1 and ABCG1 Downregulation

Synthetic LXR ligands, such as GW3965 used in the initial experiments, induce SREBP-1c, the master regulator of lipogenesis leading to fatty liver disease (Joseph et al., 2002). To circumvent this problem, a unique lipid LXR modulator *N,N*-dimethyl-3β-hydroxy-cholenamide (DMHCA) has been developed. DMHCA activates LXRs while minimally affecting SREBP-1c or activating fatty acid synthesis in the liver, kidney or intestine (Quinet et al., 2004). In our studies, treatment of BRECs with GW3965 (10 μM) and DMHCA (0.1 μM) causes a significant increase in ABCA1 and ABCG1 expression. This was accompanied by significant increase in SREBP-1c expression by GW3965 (10 μM), while DMHCA (0.1 μM) caused minimal SREBP-1c upregulation (Fig. 4c). When higher dose of DMHCA (1 μM) was used, it did induce SREBP-1c upregulation, however the effect on ABCA1 and ABCG1 upregulation was more robust when compared to GW3965 (10 μM) (Fig. 4c). To achieve maximal activation of downstream LXR targets such as ABCA1 and ABCG1, DMHCA was used at the 1 μM concentration. Future animal studies will be conducted using DMHCA at 0.1 μM to avoid potential side effects, such as lipogeneses, in vivo. As DMHCA could be a promising pharmacological agonist of LXRs, we next addressed the effectiveness of DMHCA in retinal cells. BREC were treated with 1 μM DMHCA for 24 h in the presence or absence of TNFα. Treatment with DMHCA alone caused a significant upregulation of both ABCA1 and ABCG1. Treatment with DMHCA prevented TNFα-induced downregulation of both ABCA1 and ABCG1 (Fig. 4d), suggesting that activation of LXR is sufficient to restore cholesterol efflux after TNFα stimulation in BREC. ABCA1 protein levels are significantly decreased in the presence of TNFα but LXR activation via DMHCA prevents this TNFα-induced downregulation (Fig. 4e). Interestingly, treatment with SIRT1 activator, SRT1720, does not prevent ABCA1 or ABCG1 downregulation in BREC (Supplemental Fig. 1).

3.9. Activation of the SIRT1/LXR Signaling Pathway Blocks Inflammation

Besides modulating cholesterol efflux transport pathways, LXR activation is also known to stabilize NFκB co-repressor complex preventing pro-inflammatory gene upregulation (Joseph et al., 2003). To address the effect of SIRT1/LXR modulation on inflammation, IL-1β and IL-6 were used as inflammation markers. BREC were treated with either the LXR activator DMHCA (1 μM) or SIRT1 activator SRT1720 (1 μM) for 24 h. As expected, stimulation with TNFα (10 ng/ml) caused a marked increase in IL-1β and IL-6 expression levels. Treatment with either DMHCA (Fig. 5a, c) or SRT170 (Fig. 10b, d) significantly reduced TNFα-induced IL-1β and IL-6 upregulation.

4. Discussion

As DR is a multi-faceted disease involving direct retinal cell damage by diabetic milieu, as well as infiltration of pro-inflammatory bone marrow-derived myeloid cells, and loss of function of reparative CACs in diabetes, we examined SIRT1/LXR axis in these tissues.

Activation of the LXR signaling pathway has dual beneficial consequences. First, LXR signaling has been shown to directly cause downstream activation of the RCT pathway via ABCA1 and ABCG1 activation. These membrane-associated protein transporters are the first step in the RCT pathway and are major regulators of cellular

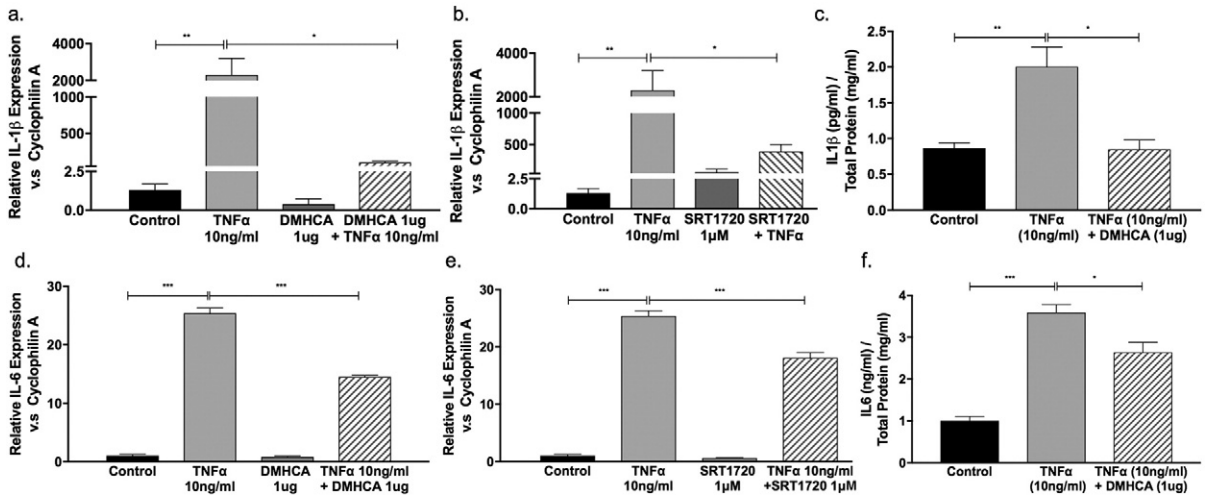

Fig. 5. LXR and SIRT1 activation blocks TNFα-induced IL-1β and IL-6 upregulation. BRECs were treated with TNFα (10 ng/ml), DMHCA (1 μM), SRT1720 (1 μM) and a combination of DMHCA (1 μM) or SRT1720 plus TNFα (10 ng/ml). Data were analyzed using qRT-PCR (a, b, d, e) and ELISA (c, f). Cyclophilin A was used as a loading control for qRT-PCR. IL-1β mRNA (a, b) and protein (c) as well as IL-6 mRNA (d, e) and protein (f) levels were significantly increased in BRECs treated with TNFα for 24 h ($n = 8$). Administration of (a, c) DMHCA or (b, e) SRT1720 for 24 h inhibited TNFα-induced IL-1β levels and IL-6 levels respectively ($n = 6$). ***$p < 0.001$ **$p < 0.01$, *$p < 0.05$.

cholesterol by acting as cholesterol efflux pumps that efflux cholesterol to lipid poor apolipoproteins (ApoA1 and ApoE) (Demina et al., 2016). The RCT pathway is actively used by the retina to transport cholesterol back to the liver in a multi-step process (Fliesler, 2015). Genetic manipulation studies have demonstrated that downregulation of ABCA1 leads to pathologic vessel thickening and hardening (Aiello et al., 2003). Loss of ABCA1 and ABCG1 also leads to accumulation of inflammatory macrophage foam cells in mice myocardium, lung, liver spleen and thymus (Yvan-Charvet et al., 2007). Additionally, individuals with ABCA1 mutations are diagnosed with Tangier disease, a disease that is characterized by a severe reduction in HDL. Activated LXR has also been shown to bind to and stabilize NCoR Complex, thus inhibiting signaling through NFκB response element on inflammatory gene promoters resulting in reduced inflammation (Huang et al., 2011).

There two LXR isoforms, LXRα and LXRβ, that are closely related sharing 80% homology in their DNA and ligand binding domains (Zhao and Dahlman-Wright, 2010). Relative expression levels of LXRα and LXRβ vary among different tissues. In the retina, both isoforms are expressed with LXRα localized to the nerve fiber layer and RPE while LXRβ is expressed in all retinal layers and RPE as well (Dwyer et al., 2011). Our previous study using STZ-induced T1D model demonstrated that enhanced LXR activity is protective against diabetes-induced retinal vascular damage, whereas LXRα$^{-/-}$ and LXRα/β$^{-/-}$ caused retinal vascular damage and development of acellular capillaries even in the absence of diabetes (Hazra et al., 2012). This study further expands these data demonstrating that LXR activation also prevented the development of acellular capillaries in T2D Lepr$^{db/db}$ model.

Importantly, HRECs isolated from diabetic donors had decreased levels of LXRα and LXRβ as compared to control tissue. To further address the role of LXR in diabetes-induced retinal endothelial cell damage, we used BREC. Inflammatory cytokines have a well-accepted role in endothelial cell damage in DR, thus we used cytokine-stimulated BREC as an in vitro model of DR (Joussen et al., 2004). BREC treated with TNFα had reduced expression level of LXRα, that was accompanied by the reduction in RCT genes ABCA1 and ABCG1, as well as upregulation of IL-1β and IL-6 expression levels. Treatment with the LXR activating ligand, DMHCA, led to significant upregulation of ABCA1 and ABCG1, and downregulation of IL-1β and IL-6 expression both in the absence and presence of TNFα. These data are in agreement with a dual role of LXR through both activation of RCT by binding to the LXR response element on ABCA1 and ABCG1 gene promoters, and in stabilizing the NCoR complex to inhibit signaling through NFκB response element on inflammatory gene promoters in retinal endothelial cells. Although both LXRα and LXRβ isoforms are expressed in retinal endothelial cells, there was a more pronounced effect of diabetes and inflammation regulated through LXRα rather than LXRβ expression.

In addition to direct effects of the diabetic metabolic milieu, activated macrophages can contribute to inflammatory conditions in the retina (Chakravarthy et al., 2016; Hazra et al., 2013). Both LXRα and LXRβ isoforms are expressed in macrophages. Activation of LXRs in macrophages suppresses the induction of inflammatory genes by LPS and leads to upregulation of RCT genes, ABCA1 and ABCG1, causing cholesterol efflux. Our data confirms that LXR activation using LXR agonist GW3965 inhibits LPS-induced cytokine production by macrophages. We further demonstrate that metabolic stimuli (palmitate, insulin, glucose) lead to reduced RCT genes (ABCA1) and increased cytokine production in the macrophages. Treatment with this LXR ligand reversed both ABCA1 inhibition and increase in IL-6 production in stimulated macrophages, strongly supporting a beneficial role of LXR activation in metabolically challenged macrophages in diabetes.

Lastly, CAC dysfunction leading to inadequate retinal vascular repair is an important contributor to DR pathogenesis. We previously demonstrated the importance of LXR signaling in CAC function using "loss of function" studies where LXRα/β$^{-/-}$ animals had significantly decreased CAC migration when compared to wild-type animals. The data presented here show that activation of LXR prevents diabetes-induced loss of CAC migration and function. Taken together, the results of this study demonstrate that LXRs are downregulated in diabetes and activation of LXR signaling has the potential to restore normal cholesterol metabolism as well as to have anti-inflammatory effects in retina and retinal cells, as well as activated macrophages and CACs, thus affecting all multiple aspects of DR pathogenesis.

It is important to note that although GW3965 activates LXR and prevents acellular capillary formation in mice, this compound has been shown to cause lipogenesis by activation of the SREBP-1c pathway leading to negative side (Quinet et al., 2004). Unlike GW3965, lipid LXR modulator DMHCA has less effect on SREBP-1, while inducing a robust activation of LXR leading to ABC upregulation (Fig. 4C). Additionally, the Quinet et al., group demonstrated that when DMHCA is administered in the presence of GW3965, DMHCA acts as a gene-selective functional antagonist and partially blocks GW3965-induced increased in SREBP-1c mRNA. Importantly, ABCA1 regulation is not affected and the ligand retains agonist properties for ABCA1 (Quinet et al., 2004). DMHCA also decreased atherosclerosis in the ApoE$^{-/-}$ mouse model

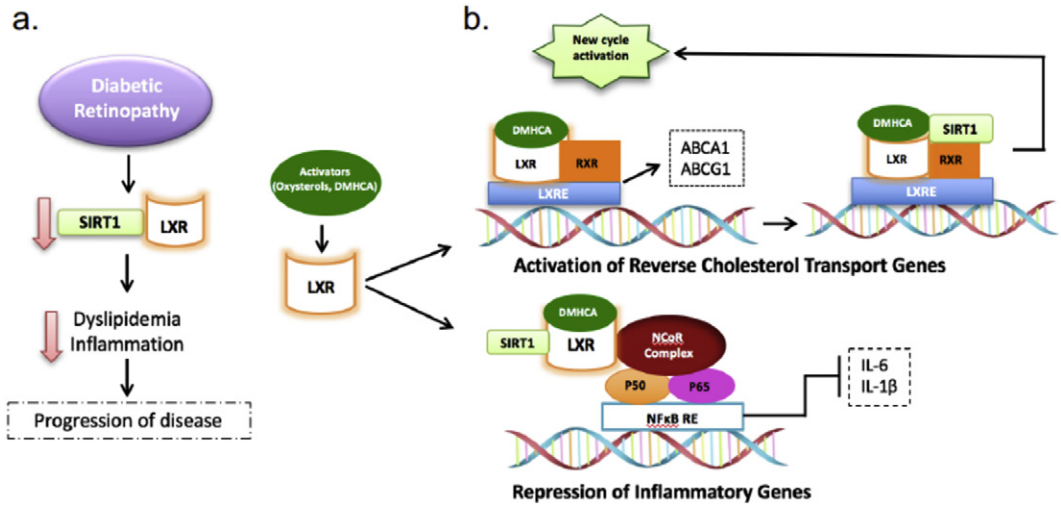

Fig. 6. Diabetes-induced decrease in SIRT1 and LXR levels results in an increase in hyperglycemia and dyslipidemia leading to progression of diabetic retinopathy (a). T2D-associated decrease in Sirt1 levels results in increased levels of acetylated LXR, which is inactive. By increasing Sirt1 levels back to nondiabetic levels, deacetylation and thus activation of LXR is facilitated. LXR activation then increases reverse cholesterol transport and represses the NFkB response element (NFkB RE) on inflammatory genes (b).

without activating fatty acid synthesis in the liver, kidney or intestine (Kratzer et al., 2009). We tested DMHCA in BREC cell culture model in this study. DMHCA was highly effective at activating LXR-dependent RCT genes and at inhibiting expression of inflammatory genes in cytokine-stimulated BREC.

Although the beneficial effects of LXR signaling have been suggested to play a key role in vascular diseases such as atherosclerosis and diabetes, the mechanism of action in which LXR activation influences inflammation and cholesterol metabolism remains an active area of investigation. LXR activity was recently shown to be controlled by acetylation at a single conserved lysine, specifically by a well-known deacetylase SIRT1 (Li et al., 2007). SIRT1 along with LXRα/β are highly expressed in retinal tissue, macrophages and CACs. SIRT1 signaling has been suggested to drive polarization of macrophages to non-inflammatory states (Purushotham et al., 2009). Moreover, mouse SIRT1 knockdown studies show significant retinal abnormalities suggesting that this enzyme plays a beneficial role in retinal development and health (Yuen et al., 2012; Kowluru et al., 2014). Recent studies suggest that SIRT1 promotes insulin secretion, reduces glucose tolerance and decreases body weight in a LXR-dependent manner (Balestrieri et al., 2013; Li et al., 2015; Zabolotny and Kim, 2007). Here, we show that cholesterol metabolism, as examined via ABCA1/ABCG1 expression levels, is significantly affected when SIRT1 is inhibited. Interestingly, LXR total levels are not affected via loss of SIRT1 suggesting that SIRT1 does not affect LXR expression levels but rather controls LXR activity. Additionally, activation of SIRT1 significantly reduces upregulation pro-inflammatory genes in retinal endothelial cells (Fig. 5).

Taken together, our studies demonstrate that type 2 diabetes has a detrimental effect on SIRT1-LXR signaling. Importantly, activation of this signaling axis not only promotes cholesterol metabolism but is also represses pro-inflammatory gene upregulation (Fig. 6). Future studies are needed to investigate the mechanism of SIRT1 activation of LXR resulting in stimulation of cholesterol metabolism pathways as well as repression of pro-inflammatory genes. These mechanistic studies will determine the best approach in which to utilize the SIRT1/LXR axis as a pharmacological target to treat DR.

Funding Sources

Research was supported by MEAS Grant MICL02163 to JVB, NIH grants: RO1EY016077 to JVB, R01EY025383 to JVB and MBG, EY012601-15, EY007739-25 to MBG, NIH DiaComp 15GHSU2550 to ML.

Conflict of Interest

The authors of this manuscripts have no conflicts of interest to disclose.

Author Contributions

All authors conducted literature searches regarding the research topic contributed to figure production by assisting in study design, data collection and analysis, and data interpretation. SSH, EB, JVB and MBG contributed by writing parts of the manuscript. SSH and JVB organized and formatted manuscript (text and figures) for submission.

Acknowledgements

We acknowledge National Research Disease Interchange and Michigan Eye-Bank for providing human retina tissue.

Appendix A. Supplementary Data

Supplementary data to this article can be found online at http://dx.doi.org/10.1016/j.ebiom.2017.07.008.

References

Aiello, R.J., Brees, D., Francone, O.L., 2003. ABCA1-deficient mice: insights into the role of monocyte lipid efflux in HDL formation and inflammation. Arterioscler. Thromb. Vasc. Biol. 23, 972–980.

Antonetti, D.A., Barber, A.J., Khin, S., Lieth, E., Tarbell, J.M., Gardner, T.W., 1998. Vascular permeability in experimental diabetes is associated with reduced endothelial occludin content: vascular endothelial growth factor decreases occludin in retinal endothelial cells. Penn State Retina Research Group. Diabetes 47, 1953–1959.

Balaiya, S., Grant, M.B., Priluck, J., Chalam, K.V., 2014. Growth factors/chemokines in diabetic vitreous and aqueous alter the function of bone marrow-derived progenitor (CD34(+)) cells in humans. Am. J. Physiol. Endocrinol. Metab. 307, E695–E702.

Balestrieri, M.L., Rienzo, M., Felice, F., Rossiello, R., Grimaldi, V., Milone, L., Casamassimi, A., Servillo, L., Farzati, B., Giovane, A., Napoli, C., 2008. High glucose downregulates endothelial progenitor cell number via SIRT1. Biochim. Biophys. Acta 1784, 936–945.

Balestrieri, M.L., Servillo, L., Esposito, A., D'onofrio, N., Giovane, A., Casale, R., Barbieri, M., Paolisso, P., Rizzo, M.R., Paolisso, G., Marfella, R., 2013. Poor glycaemic control in type 2 diabetes patients reduces endothelial progenitor cell number by influencing SIRT1 signalling via platelet-activating factor receptor activation. Diabetologia 56, 162–172.

Busik, J.V., Tikhonenko, M., Bhatwadekar, A., Opreanu, M., Yakubova, N., Caballero, S., Player, D., Nakagawa, T., Afzal, A., Kielczewski, J., Sochacki, A., Hasty, S., Li Calzi, S., Kim, S., Duclas, S.K., Segal, M.S., Guberski, D.L., Esselman, W.J., Boulton, M.E., Grant, M.B., 2009. Diabetic retinopathy is associated with bone marrow neuropathy and a depressed peripheral clock. J. Exp. Med. 206, 2897–2906.

Chakravarthy, H., Beli, E., Navitskaya, S., O'reilly, S., Wang, Q., Kady, N., Huang, C., Grant, M.B., Busik, J.V., 2016. Imbalances in mobilization and activation of pro-inflammatory

and vascular reparative bone marrow-derived cells in diabetic retinopathy. PLoS One 11, e0146829.
Coleman, D.L., 1978. Obese and diabetes: two mutant genes causing diabetes-obesity syndromes in mice. Diabetologia 14, 141–148.
Demina, E.P., Miroshnikova, V.V., Schwarzman, A.L., 2016. Role of the ABC transporters A1 and G1, key reverse cholesterol transport proteins, in atherosclerosis. Mol. Biol. (Mosk) 50, 223–230.
Dietschy, J.M., Turley, S.D., 2001. Cholesterol metabolism in the brain. Curr. Opin. Lipidol. 12, 105–112.
Du, M., Wu, M., Fu, D., Yang, S., Chen, J., Wilson, K., Lyons, T.J., 2013. Effects of modified LDL and HDL on retinal pigment epithelial cells: a role in diabetic retinopathy? Diabetologia 56, 2318–2328.
Duncan, K.G., Hosseini, K., Bailey, K.R., Yang, H., Lowe, R.J., Matthes, M.T., Kane, J.P., Lavail, M.M., Schwartz, D.M., Duncan, J.L., 2009. Expression of reverse cholesterol transport proteins ATP-binding cassette A1 (ABCA1) and scavenger receptor BI (SR-BI) in the retina and retinal pigment epithelium. Br. J. Ophthalmol. 93, 1116–1120.
Dwyer, M.A., Kazmin, D., Hu, P., Mcdonnell, D.P., Malek, G., 2011. Research resource: nuclear receptor atlas of human retinal pigment epithelial cells: potential relevance to age-related macular degeneration. Mol. Endocrinol. 25, 360–372.
Ferris III, F.L., Chew, E.Y., Hoogwerf, B.J., 1996. Serum lipids and diabetic retinopathy. Early Treatment Diabetic Retinopathy Study Research Group. Diabetes Care 19, 1291–1293.
Fliesler, S.J., 2015. Cholesterol homeostasis in the retina: seeing is believing. J. Lipid Res. 56, 1–4.
Fliesler, S.J., Bretillon, L., 2010. The ins and outs of cholesterol in the vertebrate retina. J. Lipid Res. 51, 3399–3413.
Fliesler, S.J., Florman, R., Rapp, L.M., Pittler, S.J., Keller, R.K., 1993. In vivo biosynthesis of cholesterol in the rat retina. FEBS Lett. 335, 234–238.
Hazra, S., Jarajapu, Y.P., Stepps, V., Caballero, S., Thinschmidt, J.S., Sautina, L., Bengtsson, N., Licalzi, S., Dominguez, J., Kern, T.S., Segal, M.S., Ash, J.D., Saban, D.R., Bartelmez, S.H., Grant, M.B., 2013. Long-term type 1 diabetes influences haematopoietic stem cells by reducing vascular repair potential and increasing inflammatory monocyte generation in a murine model. Diabetologia 56, 644–653.
Hazra, S., Rasheed, A., Bhatwadekar, A., Wang, X., Shaw, L.C., Patel, M., Caballero, S., Magomedova, L., Solis, N., Yan, Y., Wang, W., Thinschmidt, J.S., Verma, A., Li, Q., Levi, M., Cummins, C.L., Grant, M.B., 2012. Liver X receptor modulates diabetic retinopathy outcome in a mouse model of streptozotocin-induced diabetes. Diabetes 61, 3270–3279.
Howitz, K.T., Bitterman, K.J., Cohen, H.Y., Lamming, D.W., Lavu, S., Wood, J.G., Zipkin, R.E., Chung, P., Kisielewski, A., Zhang, L.L., Scherer, B., Sinclair, D.A., 2003. Small molecule activators of sirtuins extend *Saccharomyces cerevisiae* lifespan. Nature 425, 191–196.
Hu, P., Thinschmidt, J.S., Yan, Y., Hazra, S., Bhatwadekar, A., Caballero, S., Salazar, T., Miyan, J.A., Li, W., Derbenev, A., Zsombok, A., Tikhonenko, M., Dominguez 2nd, J.M., Mcgorray, S.P., Saban, D.R., Boulton, M.E., Busik, J.V., Raizada, M.K., Chan-Ling, T., Grant, M.B., 2013. CNS inflammation and bone marrow neuropathy in type 1 diabetes. Am. J. Pathol. 183, 1608–1620.
Huang, W., Ghisletti, S., Saijo, K., Gandhi, M., Aouadi, M., Tesz, G.J., Zhang, D.X., Yao, J., Czech, M.P., Goode, B.L., Rosenfeld, M.G., Glass, C.K., 2011. Coronin 2A mediates actin-dependent de-repression of inflammatory response genes. Nature 470, 414–418.
Janowski, B.A., Grogan, M.J., Jones, S.A., Wisely, G.B., Kliewer, S.A., Corey, E.J., Mangelsdorf, D.J., 1999. Structural requirements of ligands for the oxysterol liver X receptors LXRalpha and LXRbeta. Proc. Natl. Acad. Sci. U. S. A. 96, 266–271.
Janowski, B.A., Willy, P.J., Devi, T.R., Falck, J.R., Mangelsdorf, D.J., 1996. An oxysterol signalling pathway mediated by the nuclear receptor LXR alpha. Nature 383, 728–731.
Joseph, S.B., Castrillo, A., Laffitte, B.A., Mangelsdorf, D.J., Tontonoz, P., 2003. Reciprocal regulation of inflammation and lipid metabolism by liver X receptors. Nat. Med. 9, 213–219.
Joseph, S.B., Laffitte, B.A., Patel, P.H., Watson, M.A., Matsukuma, K.E., Walczak, R., Collins, J.L., Osborne, T.F., Tontonoz, P., 2002. Direct and indirect mechanisms for regulation of fatty acid synthase gene expression by liver X receptors. J. Biol. Chem. 277, 11019–11025.
Joussen, A.M., Poulaki, V., Le, M.L., Koizumi, K., Esser, C., Janicki, H., Schraermeyer, U., Kociok, N., Fauser, S., Kirchhof, B., Kern, T.S., Adamis, A.P., 2004. A central role for inflammation in the pathogenesis of diabetic retinopathy. FASEB J. 18, 1450–1452.
Kalaany, N.Y., Mangelsdorf, D.J., 2006. LXRS and FXR: the yin and yang of cholesterol and fat metabolism. Annu. Rev. Physiol. 68, 159–191.
Keech, A., Simes, R.J., Barter, P., Best, J., Scott, R., Taskinen, M.R., Forder, P., Pillai, A., Davis, T., Glasziou, P., Drury, P., Kesaniemi, Y.A., Sullivan, D., Hunt, D., Colman, P., D'emden, M., Whiting, M., Ehnholm, C., Laakso, M., Investigators, F.S., 2005. Effects of long-term fenofibrate therapy on cardiovascular events in 9795 people with type 2 diabetes mellitus (the FIELD study): randomised controlled trial. Lancet 366, 1849–1861.
Kern, T.S., Tang, J., Mizutani, M., Kowluru, R.A., Nagaraj, R.H., Romeo, G., Podesta, F., Lorenzi, M., 2000. Response of capillary cell death to aminoguanidine predicts the development of retinopathy: comparison of diabetes and galactosemia. Invest. Ophthalmol. Vis. Sci. 41, 3972–3978.
Kitada, M., Ogura, Y., Koya, D., 2016. The protective role of Sirt1 in vascular tissue: its relationship to vascular aging and atherosclerosis. Aging (Albany NY) 8, 2290–2307.
Klein, B.E., Klein, R., Moss, S.E., 1999. Is serum cholesterol associated with progression of diabetic retinopathy or macular edema in persons with younger-onset diabetes of long duration? Am J. Ophthalmol. 128, 652–654.
Kowluru, R.A., Santos, J.M., Zhong, Q., 2014. Sirt1, a negative regulator of matrix metalloproteinase-9 in diabetic retinopathy. Invest. Ophthalmol. Vis. Sci. 55, 5653–5660.
Kratz, M., Coats, B.R., Hisert, K.B., Hagman, D., Mutskov, V., Peris, E., Schoenfelt, K.Q., Kuzma, J.N., Larson, I., Billing, P.S., Landerholm, R.W., Crouthamel, M., Gozal, D., Hwang, S., Singh, P.K., Becker, L., 2014. Metabolic dysfunction drives a mechanistically distinct proinflammatory phenotype in adipose tissue macrophages. Cell Metab. 20, 614–625.
Kratzer, A., Buchebner, M., Pfeifer, T., Becker, T.M., Uray, G., Miyazaki, M., Miyazaki-Anzai, S., Ebner, B., Chandak, P.G., Kadam, R.S., Calayir, E., Rathke, N., Ahammer, H., Radovic, B., Trauner, M., Hoefler, G., Kompella, U.B., Fauler, G., Levi, M., Levak-Frank, S., Kostner, G.M., Kratky, D., 2009. Synthetic LXR agonist attenuates plaque formation in apoE −/− mice without inducing liver steatosis and hypertriglyceridemia. J. Lipid Res. 50, 312–326.
Laver, N.M., Robison Jr., W.G., Pfeffer, B.A., 1993. Novel procedures for isolating intact retinal vascular beds from diabetic humans and animal models. Invest. Ophthalmol. Vis. Sci. 34, 2097–2104.
Li, M., Guo, K., Vanella, L., Taketani, S., Adachi, Y., Ikehara, S., 2015. Stem cell transplantation upregulates Sirt1 and antioxidant expression, ameliorating fatty liver in type 2 diabetic mice. Int. J. Biol. Sci. 11, 472–481.
Li, X., Zhang, S., Blander, G., Tse, J.G., Krieger, M., Guarente, L., 2007. SIRT1 deacetylates and positively regulates the nuclear receptor LXR. Mol. Cell 28, 91–106.
Liang, F., Kume, S., Koya, D., 2009. SIRT1 and insulin resistance. Nat. Rev. Endocrinol. 5, 367–373.
Lydic, T.A., Busik, J.V., Reid, G.E., 2014. A monophasic extraction strategy for the simultaneous lipidome analysis of polar and nonpolar retina lipids. J. Lipid Res. 55, 1797–1809.
Lyons, T.J., Jenkins, A.J., Zheng, D., Lackland, D.T., Mcgee, D., Garvey, W.T., Klein, R.L., 2004. Diabetic retinopathy and serum lipoprotein subclasses in the DCCT/EDIC cohort. Invest. Ophthalmol. Vis. Sci. 45, 910–918.
Mast, N., Reem, R., Bederman, I., Huang, S., Dipatre, P.L., Bjorkhem, I., Pikuleva, I.A., 2011. Cholestenoic acid is an important elimination product of cholesterol in the retina: comparison of retinal cholesterol metabolism with that in the brain. Invest. Ophthalmol. Vis. Sci. 52, 594–603.
Mcdonald, J.G., Thompson, B.M., Mccrum, E.C., Russell, D.W., 2007. Extraction and analysis of sterols in biological matrices by high performance liquid chromatography electrospray ionization mass spectrometry. Methods Enzymol. 432, 145–170.
Melamud, E., Vastag, L., Rabinowitz, J.D., 2010. Metabolomic analysis and visualization engine for LC-MS data. Anal. Chem. 82, 9818–9826.
Miranda, M.X., Van Tits, L.J., Lohmann, C., Arsiwala, T., Winnik, S., Tailleux, A., Stein, S., Gomes, A.P., Suri, V., Ellis, J.L., Lutz, T.A., Hottiger, M.O., Sinclair, D.A., Auwerx, J., Schoonjans, K., Staels, B., Luscher, T.F., Matter, C.M., 2015. The Sirt1 activator SRT3025 provides atheroprotection in Apoe −/− mice by reducing hepatic Pcsk9 secretion and enhancing Ldlr expression. Eur. Heart J. 36, 51–59.
Mitchell, S.J., Martin-Montalvo, A., Mercken, E.M., Palacios, H.H., Ward, T.M., Abulwerdi, G., Minor, R.K., Vlasuk, G.P., Ellis, J.L., Sinclair, D.A., Dawson, J., Allison, D.B., Zhang, Y., Becker, K.G., Bernier, M., De Cabo, R., 2014. The SIRT1 activator SRT1720 extends lifespan and improves health of mice fed a standard diet. Cell Rep. 6, 836–843.
Ogawa, S., Lozach, J., Jepsen, K., Sawka-Verhelle, D., Perissi, V., Sasik, R., Rose, D.W., Johnson, R.S., Rosenfeld, M.G., Glass, C.K., 2004. A nuclear receptor corepressor transcriptional checkpoint controlling activator protein 1-dependent gene networks required for macrophage activation. Proc. Natl. Acad. Sci. U. S. A. 101, 14461–14466.
Opreanu, M., Tikhonenko, M., Bozack, S., Lydic, T.A., Reid, G.E., Mcsorley, K.M., Sochacki, A., Perez, G.I., Esselman, W.J., Kern, T., Kolesnick, R., Grant, M.B., Busik, J.V., 2011. The unconventional role of acid sphingomyelinase in regulation of retinal microangiopathy in diabetic human and animal models. Diabetes 60, 2370–2378.
Pascual, G., Fong, A.L., Ogawa, S., Gamliel, A., Li, A.C., Perissi, V., Rose, D.W., Willson, T.M., Rosenfeld, M.G., Glass, C.K., 2005. A SUMOylation-dependent pathway mediates transrepression of inflammatory response genes by PPAR-gamma. Nature 437, 759–763.
Pikuleva, I.A., Curcio, C.A., 2014. Cholesterol in the retina: the best is yet to come. Prog. Retin. Eye Res. 41, 64–89.
Purushotham, A., Schug, T.T., Xu, Q., Surapureddi, S., Guo, X., Li, X., 2009. Hepatocyte-specific deletion of SIRT1 alters fatty acid metabolism and results in hepatic steatosis and inflammation. Cell Metab. 9, 327–338.
Quinet, E.M., Savio, D.A., Halpern, A.R., Chen, L., Miller, C.P., Nambi, P., 2004. Gene-selective modulation by a synthetic oxysterol ligand of the liver X receptor. J. Lipid Res. 45, 1929–1942.
Stewart, E.A., Samaranayake, G.J., Browning, A.C., Hopkinson, A., Amoaku, W.M., 2011. Comparison of choroidal and retinal endothelial cells: characteristics and response to VEGF isoforms and anti-VEGF treatments. Exp. Eye Res. 93, 761–766.
Tirabassi, R.S., Flanagan, J.F., Wu, T., Kislauskis, E.H., Birckbichler, P.J., Guberski, D.L., 2004. The BBZDR/Wor rat model for investigating the complications of type 2 diabetes mellitus. ILAR J. 45, 292–302.
Tserentsoodol, N., Sztein, J., Campos, M., Gordiyenko, N.V., Fariss, R.N., Lee, J.W., Fliesler, S.J., Rodriguez, I.R., 2006. Uptake of cholesterol by the retina occurs primarily via a low density lipoprotein receptor-mediated process. Mol. Vis. 12, 1306–1318.
Veenstra, A., Liu, H., Lee, C.A., Du, Y., Tang, J., Kern, T.S., 2015. Diabetic retinopathy: retina-specific methods for maintenance of diabetic rodents and evaluation of vascular histopathology and molecular abnormalities. Curr. Protoc. Mouse Biol. 5, 247–270.
Wang, H., Han, X., Wittchen, E.S., Hartnett, M.E., 2016a. TNF-alpha mediates choroidal neovascularization by upregulating VEGF expression in RPE through ROS-dependent beta-catenin activation. Mol. Vis. 22, 116–128.
Wang, Q., Bozack, S.N., Yan, Y., Boulton, M.E., Grant, M.B., Busik, J.V., 2014. Regulation of retinal inflammation by rhythmic expression of MiR-146a in diabetic retina. Invest. Ophthalmol. Vis. Sci. 55, 3986–3994.
Wang, Q., Navitskaya, S., Chakravarthy, H., Huang, C., Kady, N., Lydic, T.A., Chen, Y.E., Yin, K.J., Powell, F.L., Martin, P.M., Grant, M.B., Busik, J.V., 2016b. Dual anti-inflammatory and anti-angiogenic action of miR-15a in diabetic retinopathy. EBioMedicine 11, 138–150.
Wang, R.H., Kim, H.S., Xiao, C., Xu, X., Gavrilova, O., Deng, C.X., 2011. Hepatic Sirt1 deficiency in mice impairs mTorc2/Akt signaling and results in hyperglycemia, oxidative damage, and insulin resistance. J. Clin. Invest. 121, 4477–4490.
Yuen, D.A., Zhang, Y., Thai, K., Spring, C., Chan, L., Guo, X., Advani, A., Sivak, J.M., Gilbert, R.E., 2012. Angiogenic dysfunction in bone marrow-derived early outgrowth cells from diabetic animals is attenuated by SIRT1 activation. Stem Cells Transl. Med. 1, 921–926.

Yvan-Charvet, L., Ranalletta, M., Wang, N., Han, S., Terasaka, N., Li, R., Welch, C., Tall, A.R., 2007. Combined deficiency of ABCA1 and ABCG1 promotes foam cell accumulation and accelerates atherosclerosis in mice. J. Clin. Invest. 117, 3900–3908.

Zabolotny, J.M., Kim, Y.B., 2007. Silencing insulin resistance through SIRT1. Cell Metab. 6, 247–249.

Zeng, H.T., Fu, Y.C., Yu, W., Lin, J.M., Zhou, L., Liu, L., Wang, W., 2013. SIRT1 prevents atherosclerosis via liverXreceptor and NFkappaB signaling in a U937 cell model. Mol. Med. Rep. 8, 23–28.

Zhao, C., Dahlman-Wright, K., 2010. Liver X receptor in cholesterol metabolism. J. Endocrinol. 204, 233–240.

Zheng, W., Reem, R.E., Omarova, S., Huang, S., Dipatre, P.L., Charvet, C.D., Curcio, C.A., Pikuleva, I.A., 2012. Spatial distribution of the pathways of cholesterol homeostasis in human retina. PLoS One 7, e37926.